AppliedChem

MDPI

Article

Towards the Reuse of Sauce By-Product: Combining Analytical Chemistry and Chemometrics to Develop New Sustainable Products

Samuele Pellacani [1], Marina Cocchi [1], Enrico Busi [2], Stefano Raimondi [2], Silvia Grassi [3], Sara Limbo [3], Serena Gobbi [3], Caterina Durante [1,*] and Lorenzo Strani [1]

[1] Department of Chemical and Geological Sciences, University of Modena and Reggio Emilia, 41125 Modena, Italy; samule.pellacani@unimore.it (S.P.); marina.cocchi@unimore.it (M.C.); lorenzo.strani@unimore.it (L.S.)
[2] Department of Life Sciences, University of Modena and Reggio Emilia, 41125 Modena, Italy; enrico.busi@unimore.it (E.B.); stefano.raimondi@unimore.it (S.R.)
[3] Department of Food, Environmental, and Nutritional Sciences (DeFENS), University of Milan, 20122 Milano, Italy; silvia.grassi@unimi.it (S.G.); sara.limbo@unimi.it (S.L.); serena.gobbi@unimi.it (S.G.)
* Correspondence: caterina.durante@unimore.it

Abstract

Food waste valorization represents a critical challenge and opportunity for sustainable food systems. This study investigated the reuse of sauce production by-products through two approaches: (i) solvent-free recovery of an oil-rich fraction and (ii) development of polymeric films for potential edible or biodegradable packaging. Centrifugation recovered approximately 10 g per 100 g of by-product. The recovered oil was characterized for total polyphenols and fatty acid composition, showing a profile consistent with vegetable oils (mainly olive oil), with minor contributions attributable to cheese and meat components. A full factorial design was used to prepare and test films and to study the effects of the three ingredients used, namely pectin, carvacrol, and sauce by-products, on their mechanical, surface, and antibacterial properties. Chemometric analysis based on principal component analysis (PCA) and regression-based modeling (multiple linear regression and response surface analysis) was applied to identify the relationships among the responses and the most influential factors. Among the tested formulations, N3 (low pectin and by-product; high carvacrol) showed the most favorable overall balance, combining the strongest antibacterial activity (mean inhibition halo diameter of 14.8 mm and 17.8 mm against *Escherichia coli* ATCC 11229 and *Staphylococcus aureus* ATCC 6538, respectively) with favorable mechanical performance, including the highest maximum force (0.53 ± 0.01 MPa) and elastic modulus, (6.8 ± 0.01 MPa) and intermediate elongation (12 ± 3%) and work at maximum force (11.9 ± 0.9 N mm).

Keywords: by-products; chemometrics; design of experiment; oil fraction; polymers

Academic Editor: Andrea Atrei

Received: 9 January 2026
Revised: 3 March 2026
Accepted: 22 April 2026
Published: 29 April 2026

1. Introduction

Food waste reduction is widely recognized as a pivotal strategy for building sustainable food systems, with clear nutritional and environmental benefits [1,2]. Despite increasing awareness, the agri-food chain still generates substantial waste, not only during primary production but also in downstream industrial processes [3]. The vegetable processing industry, particularly the tomato sector, contributes considerably to the overall food-waste stream [4]. In this context, tomato processing by-products have been reported to account for approximately 3–5% (w/w) of the incoming raw material [5], generating a

non-negligible industrial side-stream that requires appropriate management and valorization strategies. Addressing these residual streams through recovery and reuse directly supports the 2030 Agenda for Sustainable Development, particularly Sustainable Development Goal (SDG) 12. Indeed, Target 12.3 explicitly aims not only to halve retail and consumer food waste but also to reduce food losses along production and supply chains [6], thereby encompassing downstream industrial by-products such as those generated during sauce manufacturing. In parallel, the Kunming–Montreal Global Biodiversity Framework highlights food waste reduction (Target 16) as a lever to reduce pressures on biodiversity by lowering the demand for primary production and the associated use of land, water, and other resources [7]. Therefore, converting sauce by-products into new value-added products could be aligned with both supply chain loss reduction and biodiversity-oriented sustainability objectives.

Although tomato processing residues are often used as animal feed or fertilizers, they also represent valuable sources of bioactive compounds. Indeed, several studies have examined the reuse of tomato by-products, particularly peels and seeds, which are rich in phenols, ascorbic acid, and lycopene [4,5,8–11]. For example, Knoblich et al. [11] assessed the use of tomato processing by-products as poultry feed to increase carotenoid content in eggs for human consumption. Benakmoum et al. [8] reported that enriching refined oils with tomato peel and pulp increases lycopene, β-carotene, and phenol content, improving the nutritional quality of edible oils. Other work has investigated the anaerobic digestion of tomato by-products for methane production and explored the relationship between chemical composition and methane yields [9]. Furthermore, Manrich et al. [10] extracted cutin from tomato processing residues and used it to produce edible films, with pectin as a binding agent.

However, significant waste is generated not only from tomato peels and seeds but also from finished tomato-based products such as sauces and condiments. Production errors or deviations from quality standards can lead to non-compliant batches that must be discarded. This waste stream is compositionally more complex than tomato pomace because it contains tomatoes mixed with other ingredients (e.g., cheese, meat, basil, and olive oil). As a result, it can retain substantial amounts of lipid and other bioactive compounds, polyphenols, and carotenoids [12]. Therefore, if properly managed, these by-products could be considered as raw materials or semi-finished products for food, pharmaceutical, or cosmetic applications. While many valorization strategies focus on isolating specific high-value components [5], conventional solvent extraction is still widely used for recovering bioactive compounds from tomato pomace [5]. This approach has important limitations, including high solvent consumption and the generation of residual biomass that remains difficult to exploit.

Based on these considerations, the present research provides an initial investigation into the reuse of sauce by-products through two complementary routes: (i) recovery of an oil-rich fraction by centrifugation only, without organic solvent, and (ii) development of a tomato–pectin-based film for potential edible or biodegradable packaging applications. Recent reviews highlight progress and the remaining challenges for biodegradable packaging systems, including the need to balance mechanical and barrier performance with end-of-life requirements and food contact constraints [13–17]. In particular, edible films and coatings have attracted attention as environmentally friendly alternatives to conventional packaging materials [18–22].

Previous studies using tomato-derived cutin have highlighted the potential of such materials to protect food by limiting microbial growth, reducing contamination by foodborne pathogens, and potentially delivering bioactive compounds [23,24]. However, to the best of our knowledge, sauce production by-products have not yet been explored as an ingredient for this type of film. We hypothesized that sauce by-products are suit-

able for the valorization routes under study because they typically contain (i) an appreciable lipid fraction derived from added ingredients (e.g., olive oil and other fats) [12], which can be physically separated as an oil-rich phase, and (ii) a solid residue rich in tomato cell-wall material (fibers and polysaccharides) that may act as a functional filler in biopolymer matrices [5,10]. Accordingly, the recovered oil fraction was characterized for total phenolic content and fatty acid composition. For film development, a full factorial design (FFD) was applied by systematically varying the proportions of lyophilized by-product, pectin, carvacrol, and water to study their effects on the mechanical, surface and antibacterial properties.

Pectin was selected as the main film-forming biopolymer because it is widely used in the food industry as a gelling, thickening, and stabilizing agent, owing to its favorable physicochemical properties, including hydrogel-forming ability [21,25]. Beyond its conventional applications, pectin has been investigated for packaging purposes, particularly in edible coatings and films [10,21]. Du and Olsen proposed pectin-based edible films for wrapping fruits and vegetables to extend shelf life and reduce pathogen growth on food surfaces [26]. Carvacrol, a major constituent of oregano and thyme essential oils, was incorporated as an active ingredient due to its well-documented antibacterial activity against foodborne pathogens [16,27,28]. The combination of a pectin matrix with carvacrol therefore supports the development of an edible film with both structural functionality and antimicrobial potential. The developed films were then characterized in terms of carvacrol content, the chemical composition of the surface (through attenuated total reflection Fourier transform infrared spectroscopy, ATR-FTIR), mechanical properties, and antimicrobial activity. Principal component analysis (PCA) [29] was applied on the obtained dataset as an exploratory approach to highlight similarities and differences among films in terms of surface, chemical, mechanical, and antibacterial properties. Multiple linear regression (MLR) and response surface analysis [30] were then used to model the experimental outcomes and to evaluate how formulation variables and their interaction effects affect the measured responses. In this context, the present chemometric-driven approach enables a systematic exploration of the formulation space and supports the identification of influential factors and interaction patterns that would be difficult to capture by varying one ingredient at a time.

Overall, this study provides a proof-of-concept for the valorization of complex sauce production by-products and illustrates how combined chemical characterization and data-driven approach can support the circular economy's objectives and sustainable product development.

2. Materials and Methods

2.1. By-Product Samples

The by-product samples used for oil extraction and polymer film development were collected from a daily sauce production line of a food company (kept anonymous for confidentiality) specializing in the manufacture of various pasta sauces. The sampling plan (around 200 g every 8 h) followed the company's standard practice for monitoring by-products in continuous sauce processing. Each by-product sample was stored at 4 °C in a separate glass container, obtaining three different samples labeled as Sample A, Sample B, and Sample C. The samples were subsequently subjected to chemical characterization, which included determination of the pH, total phenolic content, total acidity, and fatty acid profile. All analyses were performed in triplicate.

2.2. Oil Mixture Extraction

From each glass container, a 100 g portion was thoroughly hand-mixed with a glass rod for 2 min to ensure homogenization. Each portion was then transferred into centrifuge tubes and subjected to centrifugation at 5000 rpm for 15 min at room temperature using an ALC multispeed centrifuge (PK 121, ALC International Srl, Milan, Italy). The oil phases recovered from tubes corresponding to each container were combined, yielding three distinct oil samples. This procedure was designed to assess potential heterogeneity within the daily waste sample matrix, given its high compositional complexity. From each 100 g portion of sauce by-product, approximately 10 g of oil was recovered. The resulting oil samples were then chemically characterized to determine the total polyphenols and fatty acid composition.

2.3. Production of Polymeric Films

For the preparation of the polymer films, 50 g of material coming from each glass container was combined (Figure 1a) and subjected to freeze-drying to remove water and stabilize the sample, yielding a lyophilized product (Figure 1b) for subsequent experimental phases. Lyophilization was performed using a Lio5P freeze dryer (CinquePascal, Milan, Italy) and the operative conditions are reported in Table S1, Supplementary Materials.

(**a**) (**b**)

Figure 1. Homogenized (**a**) and freeze-drying (**b**) sauce waste sample.

The production of the film was carried out using a home-made casting method, which involves the following steps:

1. Preparation of the solvent-lyophilized sauce–thickener–bactericidal solution.
2. Pouring of the solution onto suitable support materials.
3. Solvent evaporation/recovery and film deposition.
4. Film retrieval.

Operationally, the process began by weighing, in this order, pectin (used as a thickening agent), distilled water, and the lyophilized sample into a 100 mL round-bottom flask. Pectin was selected as a natural polysaccharide with recognized film-forming and thickening properties [10], while carvacrol was incorporated for its established antimicrobial activity [16,27,28].

The mixture was then stirred using a magnetic hot plate at 30 °C for 10 min. After heating was stopped, carvacrol was added while maintaining agitation. The amounts of lyophilized material, carvacrol, pectin, and water were systematically varied according to the Design of Experiments (DoE) approach described in Section 2.4. In particular, for DoE experiments, 10.0 g of each DoE film-forming solution was poured into plastic molds (internal dimensions: 10 cm × 2 cm × 0.3 cm; casting area = 20 cm^2) placed on a leveled

surface. Using a constant casting mass for all formulations ensured a consistent wet loading per unit area. Films were dried under a hood at room temperature, protected from light for 24 h, and then peeled off.

2.4. Experimental Design

DoE is a systematic method used in research and industry to optimize and improve formulation, processes, and products [31,32]. The objective of the DoE was to maximize the information obtained while minimizing the number of experimental trials. In this study, a two-level full factorial design was used to evaluate the effects of film formulation (pectin, carvacrol, and sauce by-product levels) on the measured responses, including color parameters, antibacterial activity, mechanical properties, extracted carvacrol content, and surface chemical composition (see Sections 2.5 and 2.6). Equal amounts of Samples A, B, and C were pooled prior to freeze-drying to remove water, in order to obtain a representative averaged ingredient consistent with continuous industrial practice. This pooled, freeze-dried material (hereafter referred to as the lyophilized by-product) was used as the by-product ingredient in all planned film formulations. Consequently, the DoE results describe the film's performance as a function of formulation factors using a representative pooled by-product and do not allow the attribution of mechanical/optical/antibacterial properties to individual A–C compositional differences.

The three investigated ingredients (factors) and their levels are reported in Table 1. In particular, for each factor, two levels were defined: a high level, denoted as (+), and a low level, denoted as (−). Additionally, the middle level, used for replicates and to check for the presence of a non-linear relationship between the variables and the responses, which is denoted as Level 0.

Table 1. Factors and level used in DoE experimentation.

Factors	Low Level (−)	Middle Level (0)	High Level (+)
x_1: pectin (g)	0.50	0.70	0.90
x_2: carvacrol (g)	0.05	0.175	0.30
x_3: lyophilized by-product (g)	1.0	1.50	2.0

The pectin range was selected to bracket concentrations commonly reported to form stable pectin-based cast films [10], while the carvacrol range was chosen to span literature-relevant antimicrobial loadings [26] and to extend the domain to account for potential retention/release effects introduced by the complex sauce by-product matrix. The lyophilized by-product range was defined according to preliminary formulation trials, aiming to identify practically feasible incorporation levels that maintain castability and film integrity after drying, while still producing measurable changes in the optical, mechanical, and antibacterial responses. Overall, the factor ranges were therefore selected to balance literature relevance with practical processing constraints.

Considering 3 factors at two levels, 8 different formulations were planned, along with 3 replicates of the central point, for a total of 11 experiments. The experimental plan detailing the formulations based on the selected design is reported in Table 2. A full-factorial design was feasible in this study, instead of a formulation design, because the three ingredients could vary independently. Water was used as a "filler" to ensure that the final solution in each trial weighed 10 g.

Table 2. DoE experimental plan.

N° of Experiment	Pectin (g)	Carvacrol (g)	Lyophilized By-Product (g)	Water (g)
N1	0.50	0.05	1.00	8.45
N2	0.90	0.05	1.00	8.05
N3	0.50	0.30	1.00	8.20
N4	0.90	0.30	1.00	7.80
N5	0.50	0.05	2.00	7.45
N6	0.90	0.05	2.00	7.05
N7	0.50	0.30	2.00	7.20
N8	0.90	0.30	2.00	6.80
N9	0.70	0.175	1.50	7.625
N10	0.70	0.175	1.50	7.625
N11	0.70	0.175	1.50	7.625

Each solution resulting from the DoE formulation (Table 2) was placed onto a custom-made support designed by the research team and spread evenly using a spatula to ensure consistent dimensions across all DoE trials. After drying, the films had an approximate length and thickness of 10 cm and 0.20 mm, respectively. The films' thickness was measured using a high-accuracy digital micrometer (Mitutoyo Corporation, Kawasaki, Japan; accuracy 0.001 mm). For each film, thickness was measured at five random positions, and the mean value was used for data analysis.

Table S2 in the Supplementary Materials reports the quantities used for preparing the 11 films. The films exhibited uniform thickness and the characteristic color imparted by the incorporated sauce residues. Variations in color and texture correspond to differences in formulation according to the experimental design, as described in Section 3.2.

2.5. Oil Mixtures' Characterization

2.5.1. Determination of Total Phenolic Content

Determination of the total phenolic content was carried out following the Folin–Ciocalteu method [33]. Briefly, 1 g of the oil sample was transferred into a 100 mL round-bottom flask, and 20 mL of an 80% methanol solution was added to the sample. The phenolic component extraction occurred under reflux on a water bath at 80 °C for 30 min. The obtained extract was diluted to 50 mL with an 80% methanol solution. Next, 0.5 mL of prepared extract was mixed with 5.0 mL of Folin–Ciocalteu reagent, previously diluted 1:10 with distilled water. After a 4 min reaction, 4.0 mL of a 7.5% sodium carbonate solution was added and mixed. After incubation at room temperature for 30 min, absorbance was measured at 750 nm using an Ultraspec 3000 UV spectrophotometer (Pharmacia Biotech, Uppsala, Sweden). All the processes mentioned above for the extracts were applied for the different concentrations (0.02–0.2 mg/mL) of gallic acid solution as a standard to prepare a calibration curve. Total phenolic content was expressed in grams of gallic acid per 100 g of oil (g gallic acid/100 g oil) [33]. All the measurements were carried out in triplicate.

2.5.2. Determination of the Fatty Acid Profile

For this, 1 g of the oil sample was mixed with 1 mL of a 2 M KOH–methanol solution. The mixture was heated at 70 °C for 15 min [34]. After cooling, 5 mL of n-hexane was added, and the vessel was manually shaken for 5 min. The resulting hexane layer was then filtered through a Pasteur pipette filled with anhydrous sodium sulfate. Fatty acid methyl

ester (FAME) analysis was performed using an Agilent 7890B GC System (Santa Clara, CA, USA) coupled with an Agilent HP 5973 mass spectrometer (Santa Clara, CA, USA) and equipped with a split/splitless injector. Separations were achieved using a HP-5ms ((5-phenyl)-methylpolysiloxane) capillary column (30 m × 0,25 mm × 0,25 µm). Helium was used as the carrier gas at a flow rate of 1 mL × min^{-1} and a split ratio of 1:20. The injector temperature was set at 250 °C. The oven temperature program was as follows: an initial temperature of 45 °C, increased to 240 °C at a rate of 10 °C/min and held at the final temperature for 15.5 min. Mass spectra were acquired in the m/z 25–300 range, with the MS source temperature set at 255 °C and a transfer line at 270 °C. Putative compound identification was performed using the NIST 14 (Gaithersburg, MD, USA) and Wiley 275 (Hoboken, NJ, USA) libraries. The fatty acid (FA) composition for each acid was expressed as % of total FA.

2.6. Film Characterization

2.6.1. Film Color

L*, a*, and b* coordinates were obtained performing measurements with a UV–vis/Nir V-770 spectrometer (Jasco, Tokyo, Japan). The parameters used for the measurements are reported in Table S3, Supplementary Materials. Three readings were performed for each film.

2.6.2. Attenuated Total Reflection Fourier Transform Infrared Spectroscopy (ATR-FTIR)

FTIR measurements were carried out on a FTIR Vertex spectrometer (Bruker, Ettlingen, Germany) operating in attenuate total reflection (ATR) mode. The setting parameters used are reported in Table S4, Supplementary Materials. Three readings were performed for each film. The average of the signals acquired at the three points was used for the chemometric data analysis.

2.6.3. Measurement of Carvacrol in Films by HPLC

Carvacrol content in each film was determined to gain insights into the antimicrobial properties of the developed materials. Briefly, 200 mg of each film was placed in a 20 mL vial along with 10 mL of a 25% ethanol solution [26]. The vial was sealed with parafilm to prevent solvent evaporation and left for six hours to ensure the complete release of carvacrol from the polymer matrix. After the extraction, the liquid was diluted 10-fold with acetonitrile and analyzed by HPLC (UFLC XR SHIMADZU, Tokyo, Japan).

HPLC analysis was performed on an RD-083 Hybersil C18 column (250 × 4.6 mm, 5 µm particle size) (Thermo Scientific, Waltham, MA, USA). The B mobile phase consisted of 80% acetonitrile with 0.1% phosphoric acid. Chromatographic separation was carried out under isocratic conditions. The setting parameters used are reported in Table S5, Supplementary Materials.

2.6.4. Mechanical Tests

The mechanical properties of the polymeric films were evaluated using the standard ASTM D882 method (Standard Test Method for Tensile Properties of Thin Plastic Sheeting, ASTM International, West Conshohocken, PA, USA, 2018), employing a universal testing machine (Zwick/Roell Z005, Ulm, Germany) equipped with a 5 kN load cell. The tests were conducted under controlled environmental conditions of 25 °C and 45% relative humidity (RH), with a crosshead speed of 50 mm/min. The composition of a material significantly influences its mechanical properties, such as elasticity and tensile strength. For this reason, tensile tests were performed to assess the mechanical properties of the obtained polymer films and their correlation with their composition. The following parameters were determined with the software testXpert (V11.02).

- Elastic modulus (E): This measures the material's stiffness, i.e., its elastic deformation under a given tensile force. A higher modulus indicates a stiffer and less deformable material.
- Elongation at maximum force (ε at Fmax): This quantifies how much the material can be stretched before breaking.
- Maximum force (Fmax): This represents the maximum force the material can withstand before breaking.
- Work at maximum force (W at Fmax): This measures the energy absorbed by the material upon reaching the maximum force.

These tests provided a comprehensive understanding of the films' mechanical behavior and their dependence on compositional variations.

2.6.5. Antibacterial Activity Test

The antibacterial tests of the polymer films were performed according to an adaptation of the ISO 20645:2004 method based on a Kirby–Bauer agar diffusion protocol [35]. Briefly, 7 mm disks (approx. 20 mg) of each film sample, containing the antibacterial agent carvacrol, were placed onto plates containing 15 mL of Tripticase Soy Agar (TSA; casein peptone = 15.0 g/L, soya peptone = 5.0 g/L, sodium chloride = 5.0 g/L, and agar = 15.0 g/L). A disk containing 10 µg of carvacrol was included on each plate as a positive inhibition reference. Ten milliliters of molten TSA, maintained at 45 °C, were inoculated with a fresh overnight culture of *Escherichia coli* ATCC 11,229 or *Staphylococcus aureus* ATCC 6538 to achieve a final concentration of approximately 10^6 CFU/mL and carefully poured over the agar's surface. This approach ensured that the polymer disks remained stabilized on the testing surface while allowing close contact with the bacterial lawn. Following overnight incubation at 37 °C, the presence of a clear inhibition zone around the disks indicated suppression of microbial growth and confirmed the antibacterial activity of the films. Growth inhibition was quantified by measuring the diameter of the inhibition zones, with values reported as the mean of at least three independent replicates.

2.7. Statistical Analysis

One-way analysis of variance (ANOVA) was applied to the data. Mean values were compared using Tukey's test at a confidence level of 95% ($p < 0.05$).

PCA and MLR regression were carried out by using PLSToolbox 8.9.2 software (Eigenvector Research Inc., Manson, WA, USA) for MATLAB® (version R2024b). Designs of experiments were planned with MODDE 9.1 (Umetrics AB, Umeå, Sweden).

3. Results

3.1. Chemical Characterization of By-Product Samples

The collected by-products were subjected to chemical characterization. The results, summarized in Tables 3 and 4, are consistent with those reported in previous studies on similar waste samples [12]. Considering pH, total phenols, and total acidity, the samples show differences. In particular, Sample C has a significantly higher pH ($p < 0.05$) and lower phenol content than Samples A and B, while Sample B has the highest phenol content. As regards fatty acid composition, the samples seem to be different for palmitoleic and palmitic acid contents.

Table 3. pH, total acidity, and total phenolic content (mean ± standard deviation) obtained for the sauce by-products.

	pH	Total Acidity (g Citric Acid/100 g of Dried Sauce)	Total Phenolic Content (g Gallic Acid/100 g of Dried Sauce)
Sample A	4.21 ± 0.03 a	7.3 ± 0.7 a	18.4 ± 0.2 a
Sample B	4.26 ± 0.03 a	6.0 ± 0.7 ab	22.0 ± 0.2 b
Sample C	4.67 ± 0.03 b	5.5 ± 0.7 b	17.8 ± 0.2 c

[a–c] Mean values ± standard deviations followed by equal superscript letters within the same column are not different ($p > 0.05$; one-way ANOVA followed by Tukey's post hoc test).

Table 4. Percentage of fatty acid composition, FAME, (mean ± standard deviation) obtained for the sauce by-products.

FAME	Sample A	Sample B	Sample C
Myristic acid, C14:0 (%)	0.4 ± 0.2 a	0.5 ± 0.2 a	0.4 ± 0.2 a
Palmitoleic acid, C16:1 (%)	0.4 ± 0.1 ab	0.2 ± 0.1 a	0.6 ± 0.1 b
Palmitic acid, C16:0 (%)	10.4 ± 0.5 ab	9.3 ± 0.5 a	11.0 ± 0.5 b
Linoleic acid, C18:2 (%)	6.2 ± 0.5 a	6.6 ± 0.5 a	6.2 ± 0.5 a
Oleic acid, C18:1 (%)	78 ± 2 a	80 ± 2 a	80 ± 2 a
Stearic acid, C18:0 (%)	4.1 ± 0.4 a	4.7 ± 0.4 a	3.8 ± 0.4 a
Arachidic acid, C20:0 (%)	0.4 ± 0.1 a	0.2 ± 0.1 a	0.2 ± 0.1 a
Cerotic acid (%)	0.4 ± 0.2 a	0.4 ± 0.2 a	0.4 ± 0.2 a

[a,b] Mean values ± standard deviations followed by equal superscript letters within the same row are not different ($p > 0.05$; one-way ANOVA followed by Tukey's post hoc test).

3.2. Characterization of the Oil Mixture

The overall workflow for sauce by-product valorization combining analytical chemistry and chemometrics is reported in Scheme 1.

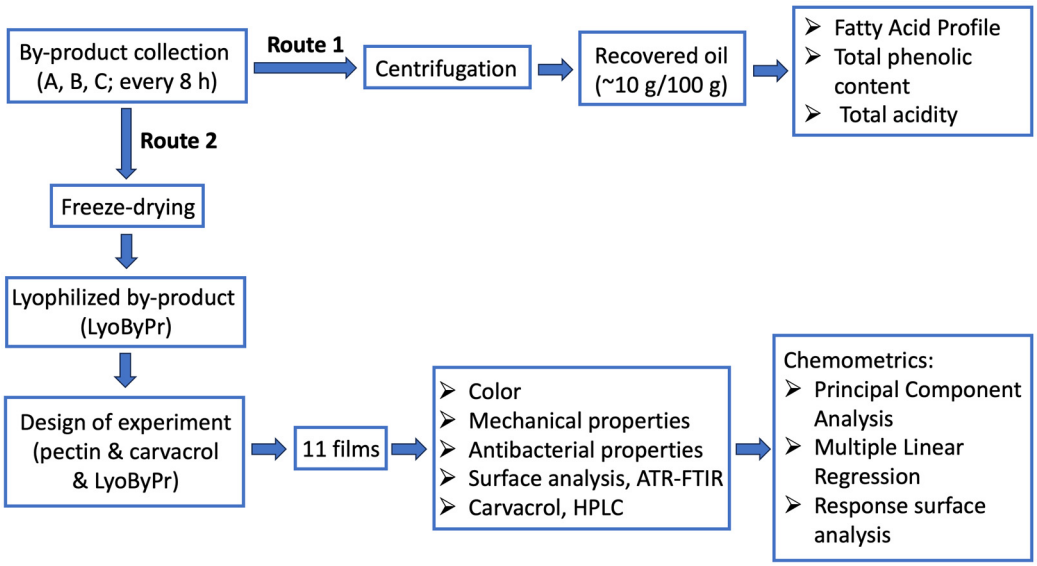

Scheme 1. Overall workflow of the study.

Total phenolic contents obtained for the extracted oils (Route 1, Scheme 1) are reported in Table 5.

Table 5. Results of total phenolic content in extracted oils (mean ± standard deviation). Total phenolic content is expressed as grams of gallic acid per 100 g of oil.

Oil	g of Oil	Total Phenolic Content (g Gallic Acid/100 g Oil)
Sample A	1.0239	1.4 ± 0.2 ab
Sample B	0.9820	1.7 ± 0.2 b
Sample C	1.0271	1.2 ± 0.2 a

[a,b] Mean values ± standard deviations followed by equal superscript letters within the same column are not different ($p > 0.05$; one-way ANOVA followed by Tukey's post hoc test).

The phenolic concentration measured in each oil sample was very low compared with the total phenolic content of the original by-product (Table 3). This may be explained by the preferential retention of phenolics in the solid phase during centrifugation, consistent with reports on the partitioning of phenolic compounds in oil-related processing systems, as reported in literature [36–38]. Since phenolics were not quantified in the post-centrifugation solid residue, a complete mass balance cannot be established, and this interpretation should be regarded as a limitation.

Fatty acid percentages obtained for each investigated oil sample are reported in Table 6.

Table 6. Concentration of fatty acids (%) in the oils extracted from Samples A, B, and C.

	% Concentration		
	Sample A	**Sample B**	**Sample C**
FAME			
Capric acid	0.21 ± 0.04 a	0.22 ± 0.03 a	0.23 ± 0.03 a
Lauric acid	0.32 ± 0.06 a	0.35 ± 0.03 a	0.35 ± 0.01 a
Myristoleic acid	0.05 ± 0.01 a	0.05 ± 0.02 a	0.07 ± 0.01 a
Myristic acid	1.5 ± 0.2 a	1.5 ± 0.3 a	1.58 ± 0.09 a
2-Methyl-decanoic acid	0.010 ± 0.003 a	0.010 ± 0.004 a	0.020 ± 0.002 b
(S)-12-methyl-tetradecanoic acid	0.030 ± 0.006 a	0.04 ± 0.01 a	0.040 ± 0.004 a
Pentadecanoic acid	0.12 ± 0.03 a	0.13 ± 0.02 a	0.14 ± 0.01 a
Palmitoleic acid	0.54 ± 0.06 a	0.55 ± 0.09 a	0.59 ± 0.05 a
Palmitic acid	12.0 ± 0.6 a	11.9 ± 1.1 a	12.1 ± 0.5 a
15-Methyl-hexadecanoic acid	0.03 ± 0.01 a	0.03 ± 0.01 a	0.04 ± 0.01 a
2-Hexyl-cyclopropaneoctanoic acid	0.05 ± 0.01 a	0.05 ± 0.01 a	0.07 ± 0.01 a
Margaric acid	0.09 ± 0.01 a	0.10 ± 0.01 a	0.10 ± 0.01 a
Linoleic acid	5.5 ± 0.2 a	5.9 ± 0.3 ab	6.1 ± 0.1 b
Oleic acid	73.9 ± 0.6 a	73.7 ± 0.9 a	72.7 ± 0.5 a
Stearic acid	5.2 ± 0.4 a	5.1 ± 0.4 a	5.5 ± 0.2 a
(Z)-11-Eicosenoic (gondoic) acid	0.09 ± 0.02 a	0.11 ± 0.02 a	0.11 ± 0.01 a
Arachidic acid	0.12 ± 0.01 a	0.15 ± 0.03 a	0.13 ± 0.01 a
Cerotic acid	0.12 ± 0.04 a	0.15 ± 0.03 a	0.15 ± 0.01 a

[a,b] Mean values ± standard deviations followed by equal superscript letters within the same row are not different ($p > 0.05$; one-way ANOVA followed by Tukey's post hoc test).

The fatty acid compositions of the extracted oils closely resemble those of virgin olive oil [39]. This finding suggests that the obtained oil fraction is mainly composed of vegetable oils, particularly olive oil, which is a key ingredient used for condiments and, consequently, is also present in the investigated non-compliant products that constitute waste from the

production process. However, the detection of capric, lauric, and myristoleic acids in the fatty acid profile is not consistent with typical vegetable oil compositions but rather corresponds to constituents commonly found in milk, dairy products, and other animal fats [40]. These fatty acids probably originate from the presence of cheese and meat in sauce by-products.

Despite the overall similarity in values, some fatty acids show significant variation among the oil samples, as indicated by the results of the ANOVA followed by Tukey's post hoc test. Specifically, capric, lauric, myristic, stearic, arachidic, and cerotic acids showed no significant differences in concentration among the three oils (p-value > 0.05). On the other hand, the contents of linoleic and 2-methyldecanoic acids differed significantly among the three different oil samples ($p < 0.05$).

Although Samples A, B, and C differed in pH, total acidity, total phenolics, and the content of selected fatty acids, oil recovery by centrifugation was essentially comparable across the three by-products, yielding approximately 10 g oil per 100 g of by-product for each sample. Therefore, within the investigated operating conditions, the compositional differences among A–C did not translate into measurable differences in extraction efficiency. However, the observed differences in the extracted oils could reflect intrinsic differences in the by-product matrix. Indeed, this variability may be linked to the fact that sampling was performed over a production day on a continuous line manufacturing different sauce formulations (e.g., pesto, ragù, and tomato-based sauces), which can differ in lipid sources and ingredient composition.

3.3. Characterization of Polymer Films

3.3.1. MLR Results

A multiple linear regression (MLR) model was developed to investigate the influence of the used ingredients (pectin, carvacrol, and sauce by-product) and their interactions on the monitored responses: the three color parameters, lightness (L*), red-green (a*), and yellow-blue (b*); the area of carvacrol obtained by HPLC investigation; microbial (halo diameters) results; and mechanical properties (Route 2, Scheme 1).

All the obtained values are reported in Table S6, Supplementary Materials.

For the development of MLR models the following equation was used

$$y = \beta_1 x_1 + \beta_2 x_2 + \beta_3 x_3 + \beta_4 x_1 x_2 + \beta_5 x_1 x_{13} + \beta_6 x_2 x_3 + e \quad (1)$$

where y represents the dependent variable (responses); β_1, β_2, and β_3 are the regression coefficients associated with the main factors pectin (x_1), carvacrol (x_2), and sauce by-product (x_3); β_4, β_5, and β_6 are the regression coefficients associated with the interaction among the factors; and e holds the residuals of the model. The statistical significance of the regression coefficients was assessed using a critical effect threshold (E_{crit}) calculated according to Equation (2)

$$E_{crit} = t_{0.95,N-J-1} \times s_y \quad (2)$$

where s_y is the model error estimated from the residuals, N is the number of experimental runs, J is the number of independent variables included in the model, and $t_{0.95,N-J-1}$ is the Student's t value at the 95% confidence level with $N - J - 1$ degrees of freedom. Regression coefficients with an absolute magnitude greater than E_{crit} were considered to be statistically significant.

All the MLR models showed good explained variance (R^2 > 72%) and the most influential factors, selected according to Equation (2), for each monitored response, are reported in Table 7. The symbols (+) and (−) correspond to the high and low level for each

factor, respectively, and they are distinguished by considering the sign of the respective regression coefficients. A positive coefficient sign indicates that the maximum response is achieved when a high value of this factor is set. Moreover, a term with a negative coefficient provides the maximum of the analytical response when a low value is considered.

Table 7. MLR significant factors, where the (+) and (−) symbols indicate the sign of the coefficient for a given factor and, therefore, the optimal level to obtain the maximum response; n.s.: not significant.

		L*	a*	b*	Carvacrol Areas	E.C. 11,229 #	S.A. 6538 ##	Fmax	ε at Fmax	E	W at Fmax
Pectin, pec	β_1	(−)	n.s.	n.s.	n.s.	n.s.	n.s.	(−)	(−)	(−)	(−)
Carvacrol, car	β_2	n.s.	n.s.	n.s.	(+)	(+)	(+)	(−)	(−)	n.s.	(−)
By-product sauce, smp	β_3	(−)	n.s.	n.s.	n.s.	n.s.	n.s.	(−)	(−)	(−)	(−)
Pec*car	β_4	n.s.	n.s.	n.s.	n.s.	n.s.	n.s.	(+)	(+)	n.s.	(+)
Pec*smp	β_5	(+)	n.s.	n.s.	n.s.	n.s.	n.s.	(+)	(+)	(+)	(+)
Car*smp	β_6	n.s.	n.s.	n.s.	(−)	n.s.	n.s.	(+)	n.s.	n.s.	(+)

Escherichia coli ATCC 11,229 halo diameters, mm; ## *Staphylococcus aureus* ATCC 6538 halo diameters, mm.

The L* parameter was significantly influenced by the amount of pectin (β_1) and by-product sauce (β_3) as the main and interaction terms. In particular, given the sign of the regression coefficient, and the trend of the response surface plot (Figure S1, Supplementary Materials), it increased with the decrease in the amount of sauce by-product. On the other hand, the a* and b* parameters did not show significant dependence on any factor or interaction. These findings highlighted how the visual properties of the polymer films could be fine-tuned by varying the quantity of the sauce by-product. It is worth highlighting that an optimal response does not exist, since it depends on the potential use of the films. The insights provided by the MLR model could only guide the formulation of materials with tailored aesthetic and functional attributes.

As regards carvacrol peak area, the only two significant terms were carvacrol (β_2) and its interaction with by-product sauce (β_6), with positive and negative signs, respectively. From these results and response surface plot (Figure S2, Supplementary Materials), it was observed that the amount of carvacrol extracted from the polymers was directly proportional to the amount of carvacrol present in the formulation (positive β_2 coefficient) but inversely correlated with the amount of sauce by-product. In fact, polymers N3 and N4 showed higher peak areas (Table S6, Supplementary Materials) than polymers N7 and N8, despite containing the same amount of carvacrol, as they were prepared using only half the amount of sauce waste. This could suggest that carvacrol might be trapped within the polymeric matrix by components present in the sauce. Considering that previous studies [12] identified the presence of lycopene in the sauce by-products analyzed, it is plausible to hypothesize that an increase in lycopene concentration may favor the formation of micelles with carvacrol, reducing its release [41]. However, this hypothesis requires further investigation through in-depth structural and molecular characterization of the films.

Antimicrobial activity against the two investigated bacteria seemed to be mainly influenced by the amount of carvacrol (with a positive β_3), and this result is explained in more detail in Section 3.3.2.

Finally, all the used ingredients influenced almost all the investigated mechanical properties as the main and interaction terms. Therefore, a deeper discussion of the respective results is reported in Section 3.3.3.

3.3.2. Antimicrobial Activities of Films

The antimicrobial activity of the synthesized polymer films was assessed against the foodborne pathogens *Escherichia coli* (Gram−) and *Staphylococcus aureus* (Gram+), both known to be inhibited by carvacrol [42,43]. Despite the presence of carvacrol in all formulations, some films did not show antibacterial effects. By way of example, the inhibition of the growth of *Staphylococcus aureus* ATCC 6538 on petri dishes in the presence of different film specimens (N1–N11) is reported in Figure 2.

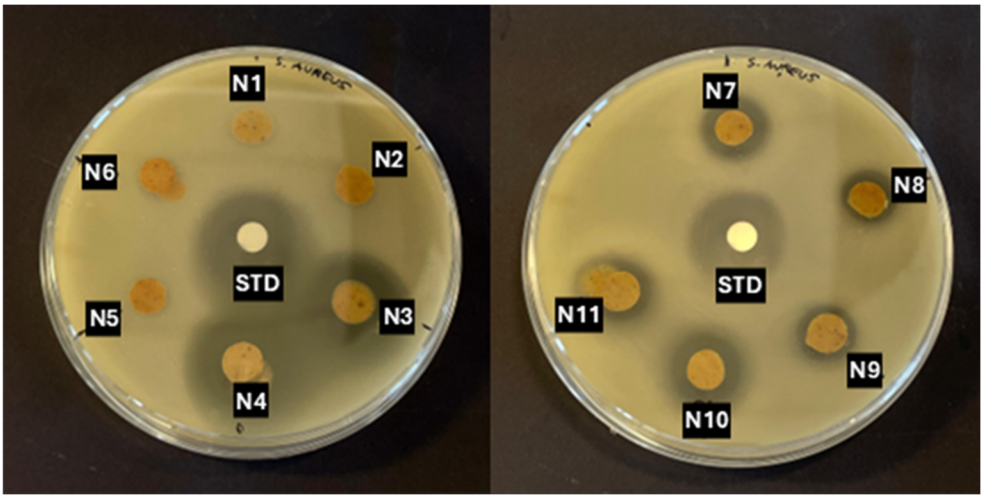

Figure 2. Growth inhibition of *Staphylococcus aureus* ATCC 6538 on petri dishes in the presence of different polymer film samples (N1–N11), tested as disks 7 mm in diameter and approximately 20 mg in weight. As a reference, 10 µg of carvacrol was applied at the center of each plate.

Specifically, Samples N1, N2, N5, and N6, which contained the lowest levels of the active compound, failed to produce inhibition halos, suggesting that carvacrol did not reach effective concentrations in the culture medium. In contrast, the other films generated distinct inhibition zones ranging from 7 to 15 mm (Figure 3a,b).

Similar results were reported by Du et al. [26], who showed that carvacrol-containing tomato-based edible films inhibited the growth of *E. coli* O157\:H7 in a concentration-dependent manner. Among the most active formulations, higher loadings of lyophilized sauce by-product material appeared to reduce efficacy, as Samples N3 and N4 produced significantly larger halos than N7 and N8, despite containing equal amounts of carvacrol. This effect may reflect a lower immediate availability of the compound, possibly due to interactions with the matrix. Such behavior could also indicate the delayed release and stabilization of carvacrol over time, as observed in nanocomposite films with nanoclays, where the filler protected carvacrol from thermal degradation and slowed its release while preserving antimicrobial activity [44]. If confirmed, this mechanism could represent a valuable feature to enhance the long-term performance of waste-based films in active packaging.

These behaviors match with chromatographic analyses, which confirmed a direct correlation between carvacrol release and antimicrobial activity. Samples N1, N2, N5, and N6, characterized by minimal release, exhibited negligible inhibition, whereas N7–N11 released comparable amounts of carvacrol and produced similar inhibition zones. Notably, N3 and N4, which showed the highest release values, also displayed the strongest antibacterial activity. Overall, these findings indicate that both the amount and bioavailability of carvacrol are critical determinants of the antimicrobial performance of the films.

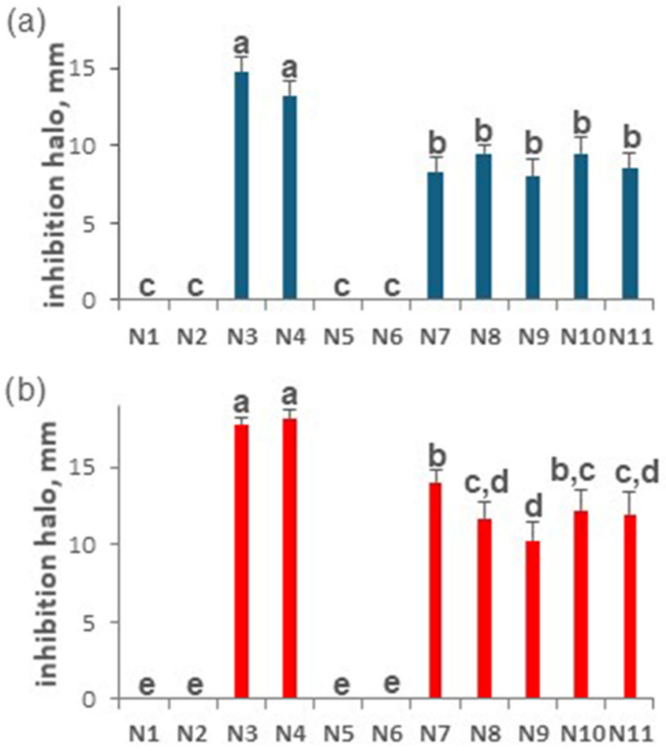

Figure 3. Antimicrobial activity of polymeric films N1–N11 against *E. coli* ATCC 11,229 (**a**) and *S. aureus* ATCC 6538 (**b**). Values are the mean inhibition halo diameters (mm, $n \geq 3$). Bars with the same letter are not significantly different ($p > 0.05$; one-way ANOVA followed by Tukey's post hoc test).

3.3.3. Mechanical Test Results

No mechanical data were obtained for Sample N1 because the specimen fractured during mounting due to its extremely brittle behavior. Notably, N1 corresponds to the lowest levels of pectin, carvacrol, and sauce by-product in the factorial design. Visual inspection revealed numerous defects (e.g., microvoids/holes), indicating poor matrix continuity. Such microdefects act as stress concentrators and can trigger premature failure, rationalizing the inability to test N1 under tensile loading. For all the other films, the parameters measured included maximum force (Fmax), strain at maximum force (ε at Fmax), Young's modulus (E), and work at maximum force (W at Fmax). The results of these measurements are reported in Table 8.

Table 8. Results of mechanical tensile tests performed on the samples.

Samples	F max (MPa)	ε at Fmax (%)	E (MPa)	W at Fmax (Nmm)
N1	-	-	-	-
N2	0.50 ± 0.01	11 ± 3	5.6 ± 0.1	16.2 ± 0.9
N3	0.53 ± 0.01	12 ± 3	6.8 ± 0.1	11.9 ± 0.9
N4	0.15 ± 0.01	4 ± 3	5.4 ± 0.1	1.5 ± 0.9
N5	0.17 ± 0.01	14 ± 3	1.7 ± 0.1	4.3 ± 0.9
N6	0.21 ± 0.01	15 ± 3	3.0 ± 0.1	5.7 ± 0.9
N7	0.06 ± 0.01	4 ± 3	1.4 ± 0.1	0.5 ± 0.9
N8	0.39 ± 0.01	14 ± 3	4.4 ± 0.1	17.6 ± 0.9
N9	0.45 ± 0.01	15 ± 3	5.9 ± 0.1	10.7 ± 0.9
N10	0.44 ± 0.01	16 ± 3	5.8 ± 0.1	9.7 ± 0.9
N11	0.43 ± 0.01	14 ± 3	5.7 ± 0.1	8.9 ± 0.9

The mechanical performance of the developed films (Fmax = 0.06–0.53 MPa; E = 1.4–1.6 MPa; ε at Fmax = 4–16%) is markedly lower in strength and stiffness than tomato-derived edible films reported in the literature [10,26]. For example, Du et al. [26] reported tomato puree films containing carvacrol with a tensile strength of 8.9–14.8 MPa and an elongation of 6.0–11.6%, depending on the casting method and carvacrol concentration. Similarly, Manrich et al. [10] reported cutin/pectin films with a tensile strength of 9.6–36.7 MPa and low elongation at break (0.4–4.0%). Overall, compared with these reference systems, the films developed in this study fall within a different mechanical regime, while maintaining elongation values in the same order of magnitude as carvacrol-containing tomato puree films. Indeed, according to the results reported in Table 8, almost all polymers (except polymers N4 and N7) exhibited an elongation at the maximum force (ε at Fmax) higher than 11%. Sample N8 additionally absorbed the greatest amount of energy once the maximum force was reached. Film N3 showed the greatest resistance and stiffness, as it required the highest force (Fmax) to break and was characterized by the highest Young's modulus. N7 showed the lowest values for all the variables considered. Film N4, which, together with N3, was particularly relevant in the biological analyses, in this case exhibited intermediate values of elastic modulus and showed a behavior similar to N7 with respect to the other parameters.

The mechanical properties of edible films were modeled using multiple linear regression, MLR. For each response, models were estimated, including the main terms associated with the formulation factors (carvacrol, pectin, and grams of by-product) and two-term interactions (Equation (1)). In all of the obtained models (Table 7), the main terms are statistically significant and associated with negative regression coefficients, indicating that an increase in the level of each factor tends to reduce the mechanical response. A high level of the factors studied could lead to a decrease in the continuity and cohesion of the matrix and/or an increase in microstructural defects (e.g., microheterogeneity, voids or microcracks) [36,45]. It is important to emphasize that the main negative effects should be interpreted as trends within the domain studied and do not necessarily imply that each ingredient is inherently harmful under all conditions. At the same time, statistically significant positive interactions between two factors indicate a non-additive response. In particular, the negative effect of one factor may be partially mitigated when another factor is simultaneously increased or decreased. This model suggests the presence of synergistic or compensatory mechanisms related to the formulation-dependent microstructure, such as improved dispersion/stabilization of the hydrophobic phase and/or improved stress distribution when two components vary together. Unfortunately, it was not possible to obtain response surface plots in this case, since during mechanical characterization, the formulation corresponding to the lowest level of all factors (sample N1) showed decidedly fragile behavior, fracturing during specimen handling prior to the tensile test. Although this prevented the determination of the modulus E, ε at Fmax, Fmax, and W at Fmax for that formulation, this event should not be considered a loss of data; rather, it provides experimental evidence of insufficient structural integrity in that region (a low level for all the three factors) of the formulation space. This behavior is consistent with the coefficient pattern observed in the MLR models (negative main effects coupled with positive two-factor interactions), which points to a strongly non-additive system where performance depends on the combined balance of ingredients rather than on single factors alone. A plausible, verifiable interpretation is that at low pectin/low by-product, the film may exhibit lower matrix continuity and/or higher sensitivity to local defects (e.g., thickness variability or drying-induced micro-heterogeneities), making it more prone to stress concentrations at the grips. These interpretations remain verifiable mechanistic hypotheses and need to be

further supported, for example, by measuring the variability in thickness and observing the microstructure through optical microscopy or SEM analysis.

To obtain a more comprehensive overview of the relationships among the measured responses, PCA was also applied to the data matrix including color parameters, antibacterial results, mechanical properties, and the HPLC carvacrol peak area for the investigated films. Sample N1 was excluded from this analysis because mechanical data were not available, resulting in a dataset of 10 films. The data were autoscaled, and a two principal component model was selected, based on the lowest RMSECV (leave-one-out), and the retained components explained 81% of the total variance. Figure 4 shows the corresponding biplot, where film samples are reported as red symbols and the measured variables as blue symbols.

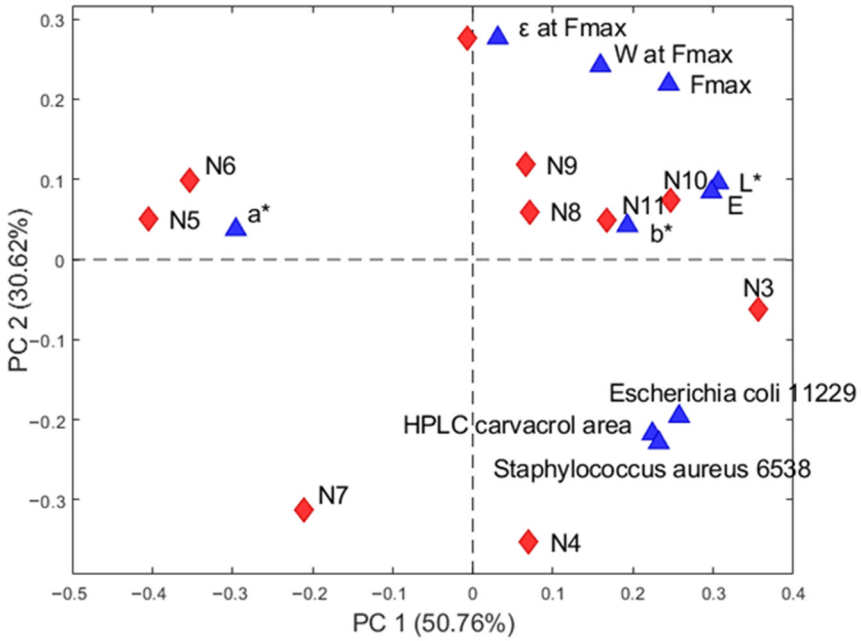

Figure 4. PC1 vs. PC2 biplot of PCA analysis applied to the data matrix including color parameters (a*, b* and L*), antibacterial results (*Escherichia coli* 11,229 and *Staphylococcus aureus* 6538), mechanical properties (Fmax, E, ε at Fmax, and W at Fmax), and the HPLC carvacrol peak area (HPLC carvacrol area) for the investigated films.

N3 and N4 are located in the lower right quadrant (positive PC1 and negative PC2). Both films are associated with a high carvacrol HPLC peak area, which, as expected, is closely aligned with the antibacterial variables in the biplot, indicating a direct relationship between carvacrol content and antimicrobial performance. In contrast, N2 (high pectin, low carvacrol, and low by-product) is separated mainly along the positive PC2 and is associated with relatively high values for most mechanical properties.

Regarding the color variables, all monitored responses show positive PC1 loadings, except for a*, which shows negative PC1 loadings. This indicates that a* captures a variability trend opposite to the general pattern described by the other responses. Furthermore, a* is closer to samples N5 and N6, suggesting that these formulations are characterized by relatively higher a* values compared with the other films. PC2 is the component that primarily discriminates between antibacterial performance, mainly associated with positive PC1 and negative PC2 loadings, and mechanical responses (ε and W at Fmax, and Fmax) mainly associated with both positive PC1 and PC2 loadings. In this framework, L*, E, and b* show positive PC1 loadings but PC2 values close to zero, suggesting that these

descriptors are not strongly aligned with either the antibacterial (negative PC2) or the mechanical performance (positive PC2) directions.

Considering the need to identify a compromise between mechanical performance (mainly associated with positive PC2) and antibacterial performance (mainly associated with positive PC1 and negative PC2), N3 appears to provide the most balanced profile. Specifically, N3 maintains positive PC1 values while exhibiting higher PC2 scores than N4, suggesting improved mechanical behavior at comparable antimicrobial potential. Overall, these multivariate trends are consistent with the conclusions drawn from the MLR models, supporting the identification of N3 as a promising formulation within the investigated experimental domain.

3.3.4. ATR-FTIR Characterization

ATR-FTIR spectra obtained from the polymeric films produced according to the different formulations planned within the DoE approach are reported in Figure 5.

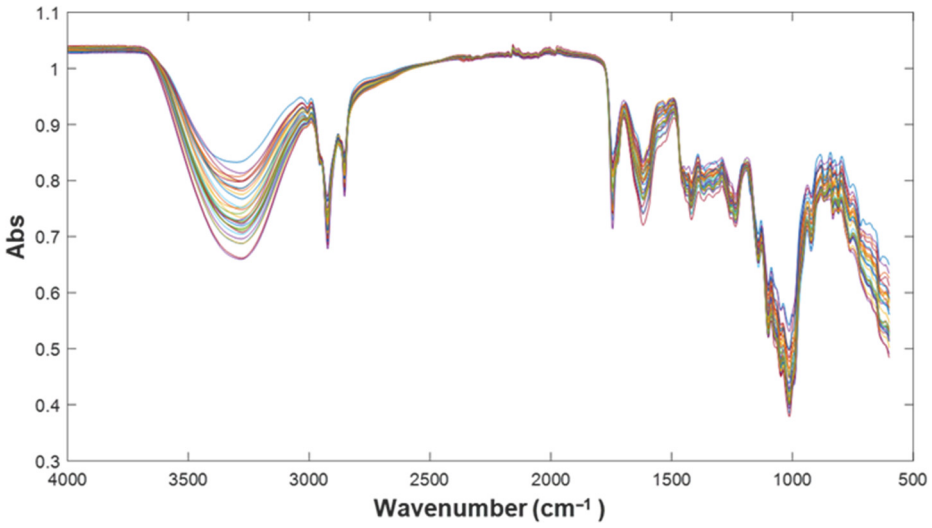

Figure 5. ATR-FTIR spectra of polymeric films.

The fingerprint spectra of the analyzed samples present characteristic bands mainly attributable to cutin [10], namely the ones around 1730 cm^{-1} (ester vibrations) and in the region of 2950–2850 cm^{-1} (stretching vibrations of –CH, $–CH_2$, and $–CH_3$ groups). The bands observed between 1200 and 1500 cm^{-1} are typical of deformation vibrations of C–OH groups in carbohydrates, likely related to the presence of pectin [10]. The band in the range of 1155–1100 cm^{-1} may be associated with the stretching vibrations of C–O bonds in alcohols. The broad peak around 3250 cm^{-1} could be attributed to the O–H stretching vibrations of phenols, alcohols, or water. Finally, several bands between 1400 cm^{-1} and 1600 cm^{-1} could likely be assigned to functional groups of phenolic and flavonoid compounds [10].

A principal component analysis (PCA) was performed on the ATR-FTIR spectra in order to gain insight into the similarities and differences among the samples based on their surface composition. Specifically, the spectra were organized into a dataset with dimensions of 11 × 1762 (number of films × number wavelength) and mean centered before PCA analysis. The model was built considering two principal components (explained variance, R2: 94.62%). The scores plot of PC1 versus PC2 is shown in Figure 6 and highlights both similarities and differences among the films based on their ATR-FTIR spectra, reflecting the influence of the formulation on surface composition.

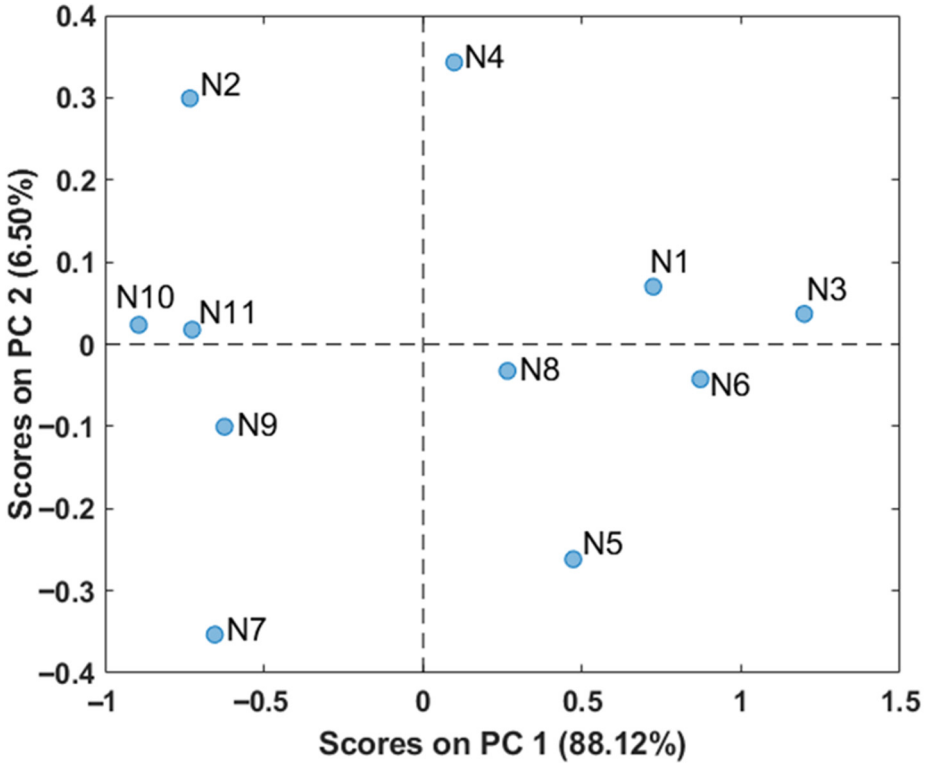

Figure 6. Score plot of PC1 vs. PC2 of the PCA model applied to the ATR-FTIR data.

From the figure, it can be observed that the replicated samples N9, N10, and N11 show good reproducibility, as they are well clustered in the same score space. Film specimens N1, N3, and N6 are separated from the others with positive PC1 scores, while N2 and N4 are different along the PC2 scores. Samples N3 and N4, with similar microbial activities, appear to be different, since N3 (high level for carvacrol and low for pectin and by-product) presents the highest PC1 score value, while N4 (high level for pectin, and low for carvacrol and by-product) presents the highest PC2 score values. The bands most responsible for the variance captured by PC1 (loadings plot in Figure 7a) are located in the 3500–3000 cm^{-1} range, around 1730 cm^{-1} and 1000 cm^{-1}, which are characteristic bands of phenol, water, and alcohols as well. Bands in the 1500–1200 cm^{-1} region, characteristic of pectin (loadings plot in Figure 7b), seem to be the most responsible for the variance captured by PC2.

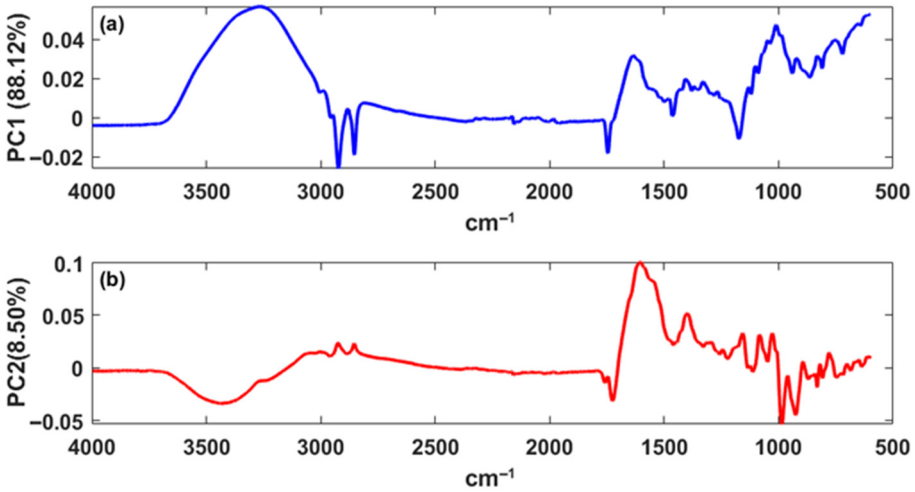

Figure 7. Loadings plot of PC1 (**a**) and PC2 (**b**) of the PCA model applied to the AT-FTIR data.

Samples N2 and N4, with the highest PC2 scores, seem to differ from the others, primarily due to bands in the 1500–1200 cm^{-1} region (loadings plot in Figure 7b), characteristic of pectin. This separation is consistent with their formulation, as both films were prepared with the highest amount of pectin. Although Sample N6 was also formulated with a high amount of pectin, it does not cluster with N2 and N4. Instead, it shows distinct spectral characteristics, likely due to its higher content of sauce by-product compared with the latter samples. This compositional difference plausibly results in a greater contribution of phenols and other organic compounds, which, in turn, modify the ATR-FTIR profile.

4. Conclusions

This study provides a preliminary proof-of-concept for the valorization of sauce production by-products, addressing both the environmental challenge of food waste and the need for innovative reuse strategies. Two exploratory routes were investigated: (i) the recovery of an oil-rich fraction by solvent-free centrifugation and (ii) the pilot development of polymer films incorporating the sauce by-product.

The fatty acid profile of the recovered oils was mainly consistent with the presence of vegetable oils, particularly olive oil, which is a key ingredient used in sauce formulation and are therefore expected to be present in non-compliant products generated along the production process.

With regard to edible films, this study indicates that sauce by-products can be incorporated into pectin-based matrices to obtain self-standing film prototypes, suggesting potential relevance for edible and/or biodegradable packaging applications. Importantly, the use of an experimental design approach enabled a systematic screening of the formulation parameters and their interactions, highlighting the importance of considering factors in an integrated rather than a one-factor-at-a-time manner. Within the investigated experimental domain, Formulation N3 emerged as the most promising candidate when antibacterial and mechanical responses were jointly considered. From an antibacterial perspective, N3 and N4 showed the highest activity, being associated with higher carvacrol content and higher by-product loadings, whereas pectin percentage appeared to have a limited influence within the tested range. However, when mechanical properties were also considered, N3, formulated with a lower pectin level, provided the most favorable overall balance among the tested films, with the highest maximum force and elastic modulus and intermediate values of elongation and work at maximum force.

However, several limitations should be acknowledged. First, a comprehensive assessment of packaging potential requires barrier characterization; therefore, water vapor permeability and oxygen permeability measurements should be included in future work. Second, the transfer of laboratory procedures to industrial contexts, particularly for oil recovery, will require dedicated evaluation. At larger scale, the higher volume and heterogeneity of the waste stream may affect the process's performance and product consistency; moreover, industrial implementation would likely require disc-stack centrifugation and process optimization. Future studies should therefore include a larger number of samples to better quantify by-product variability and apply experimental design approaches to optimize both oil recovery and film formulation under industrially relevant conditions. Advancing along these lines may contribute to reducing food waste and supporting circular economy strategies through the development of higher-value products from agri-food by-products.

Supplementary Materials: The following supporting information can be downloaded at https://www.mdpi.com/article/10.3390/appliedchem6020027/s1.

Author Contributions: Conceptualization, C.D. and M.C.; methodology, C.D., S.R., S.L. and S.P.; software, L.S.; validation, S.P., L.S., S.L. and S.R.; formal analysis, S.P., S.L., L.S. and S.G. (Serena Gobbi); investigation, S.P., S.L., E.B. and S.G. (Serena Gobbi); data curation, C.D., S.R., S.P. and M.C.; writing—original draft preparation, C.D., S.P., S.R., S.G. (Silvia Grassi) and S.L.; visualization, S.G. (Silvia Grassi) and L.S.; supervision, C.D., S.R., M.C. and S.L.; project administration, C.D. All authors have read and agreed to the published version of the manuscript.

Funding: This research received no external funding.

Institutional Review Board Statement: Not applicable.

Informed Consent Statement: Not applicable.

Data Availability Statement: The original contributions presented in this study are included in the article/Supplementary Material. Further inquiries can be directed to the corresponding author.

Conflicts of Interest: The authors declare no conflicts of interest.

References

1. Lu, Z.; Wang, J.; Gao, R.; Ye, F.; Zhao, G. Sustainable valorisation of tomato pomace: A comprehensive review. *Trends Food Sci. Technol.* **2019**, *86*, 172–187. [CrossRef]
2. Bajželj, B.; Quested, T.E.; Röös, E.; Swannell, R.P.J. The role of reducing food waste for resilient food systems. *Ecosyst. Serv.* **2020**, *45*, 101140. [CrossRef]
3. Ezeorba, T.P.C.; Okeke, E.S.; Mayel, M.H.; Nwuche, C.O.; Ezike, T.C. Recent advances in biotechnological valorization of agro-food wastes (AFW): Optimizing integrated approaches for sustainable biorefinery and circular bioeconomy. *Bioresour. Technol. Rep.* **2024**, *26*, 101823. [CrossRef]
4. Coelho, M.C.; Rodrigues, A.S.; Teixeira, J.A.; Pintado, M.E. Integral valorisation of tomato by-products towards bioactive compounds recovery: Human health benefits. *Food Chem.* **2023**, *410*, 135319. [CrossRef]
5. Eslami, E.; Carpentieri, S.; Pataro, G.; Ferrari, G. A Comprehensive Overview of Tomato Processing By-Product Valorization by Conventional Methods versus Emerging Technologies. *Foods* **2023**, *12*, 166. [CrossRef]
6. Manzoor, S.; Fayaz, U.; Dar, A.H.; Dash, K.K.; Shams, R.; Bashir, I.; Pandey, V.K.; Abdi, G. Sustainable development goals through reducing food loss and food waste: A comprehensive review. *Future Foods* **2024**, *9*, 100362. [CrossRef]
7. Hughes, A.C.; Grumbine, R.E. The Kunming-Montreal Global Biodiversity Framework: What it does and does not do, and how to improve it. *Front. Environ. Sci.* **2023**, *11*, 1281536. [CrossRef]
8. Benakmoum, A.; Abbeddou, S.; Ammouche, A.; Kefalas, P.; Gerasopoulos, D. Valorisation of low quality edible oil with tomato peel waste. *Food Chem.* **2008**, *110*, 684–690. [CrossRef]
9. Giannelos, P.N.; Sxizas, S.; Lois, E.; Zannikos, F.; Anastopoulos, G. Physical, chemical and fuel related properties of tomato seed oil for evaluating its direct use in diesel engines. *Ind. Crop. Prod.* **2005**, *22*, 193–199. [CrossRef]
10. Manrich, A.; Moreira, F.K.V.; Otoni, C.G.; Lorevice, M.V.; Martins, M.A.; Mattoso, L.H.C. Hydrophobic edible films made up of tomato cutin and pectin. *Carbohydr. Polym.* **2017**, *164*, 83–91. [CrossRef]
11. Knoblich, M.; Anderson, B.; Latshaw, D. Analyses of tomato peel and seed byproducts and their use as a source of carotenoids. *J. Sci. Food Agric.* **2005**, *85*, 1166–1170. [CrossRef]
12. Strani, L.; Farioli, G.; Cocchi, M.; Durante, C.; Olarini, A.; Pellacani, S. Chemical Characterization and Temporal Variability of Pasta Condiment By-Products for Sustainable Waste Management. *Foods* **2024**, *13*, 3018. [CrossRef]
13. Kumar, A.; Kumar, A.; Wei, S.; Chopra, S.; Rudra, S.G.; Rabbani, A. Biodegradable and smart packaging films for food quality and safety: A review. *Appl. Food Res.* **2025**, *5*, 101491. [CrossRef]
14. Jahangiri, F.; Mohanty, A.K.; Misra, M. Sustainable biodegradable coatings for food packaging: Challenges and opportunities. *Green Chem.* **2024**, *26*, 4934. [CrossRef]
15. Ali, M.Q.; Ahmad, N.; Azhar, M.A.; Munaim, M.S.A.; Hussain, A.; Mahdi, A.A. An overview: Exploring the potential of fruit and vegetable waste and by-products in food biodegradable packaging. *Discov. Food* **2024**, *4*, 130. [CrossRef]
16. Devi, L.S.; Das, B.; Dutta, D.; Kumar, S. Essential oils as functional agents in biopolymer-based sustainable food packaging system: A review. *Sustain. Chem. Pharm.* **2024**, *39*, 101563. [CrossRef]
17. Genovese, J.; Martins, D.M.; Silvetti, T.; Brasca, M.; Fracassetti, D.; Borgonovo, G.; Mazzini, S.; Limbo, S. Development of photo-active chitosan-based films with riboflavin for enhanced antimicrobial food packaging applications. *Molecules* **2025**, *30*, 4166. [CrossRef]

18. Gaspar, M.C.; Braga, M.E.M. Edible films and coatings based on agrifood residues: A new trend in the food packaging research. *Curr. Opin. Food Sci.* **2023**, *50*, 101006. [CrossRef]
19. Gupta, D.; Lall, A.; Kumar, S.; Patil, T.D.; Gaikwad, K.K. Plant-based edible films and coatings for food-packaging applications: Recent advances, applications, and trends. *Sustain. Food Technol.* **2024**, *2*, 1428. [CrossRef]
20. Oliveira, I.; Pinto, T.; Afonso, S.; Karaś, M.; Szymanowska, U.; Gonçalves, B.; Vilela, A. Sustainability in Bio-Based Edible Films, Coatings, and Packaging for Small Fruits. *Appl. Sci.* **2025**, *15*, 1462. [CrossRef]
21. Syarifuddin, A.; Muflih, M.H.; Izzah, N.; Fadillah, U.; Ainani, A.F.; Dirpan, A. Pectin-based edible films and coatings: From extraction to application on food packaging towards circular economy- A review. *Carbohydr. Polym. Technol. Appl.* **2025**, *9*, 100680. [CrossRef]
22. Liyanapathiranage, A.; Dassanayake, R.S.; Gamage, A.; Karri, R.R.; Manamperi, A.; Evon, P.; Jayakodi, Y.; Madhujith, T.; Merah, O. Recent Developments in Edible Films and Coatings for Fruits and Vegetables. *Coatings* **2023**, *13*, 1177. [CrossRef]
23. Di Matteo, A.; Stanzione, M.; Orlo, E.; Russo, C.; Lavorgna, M.; Buonocore, G.G.; Isidori, M. Biodegradable films enriched with thymol and carvacrol with antioxidant and antibacterial properties to extend cheese shelf-life. *Food Control* **2026**, *179*, 111541. [CrossRef]
24. Pié-Amill, A.; Colás-Medà, P.; Viñas, I.; Falcó, I.; Alegre, I. Efficacy of an Edible Coating with Carvacrol and Citral in Frozen Strawberries and Blueberries to Control Foodborne Pathogens. *Foods* **2024**, *13*, 3167. [CrossRef] [PubMed]
25. Douglas, T.; Hempel, U.; Zydek, J.; Vladescu, A.; Pietryga, K.; Kaeswurm, J.; Buchweitz, M.; Surmenev, R.; Surmeneva, M.; Cotrut, C. Pectin Coatings on Titanium Alloy Scaffolds Produced by Additive Manufacturing: Promotion of Human Bone Marrow Stromal Cell Proliferation. *Mater. Lett.* **2018**, *227*, 225–228. [CrossRef]
26. Du, W.-X.; Olsen, C.W.; Avena-Bustillos, R.J.; McHugh, T.H.; Levin, C.E.; Friedman, M. Antibacterial Activity against E. coli O157:H7, Physical Properties, and Storage Stability of Novel Carvacrol-Containing Edible Tomato Films. *J. Food Sci.* **2008**, *73*, M378–M383. [CrossRef]
27. Friedman, M.; Henika, P.R.; Levin, C.E.; Mandrell, R.E. Antibacterial activities of plant essential oils and their components against Escherichia coli O157:H7 and Salmonella enterica in apple juice. *J. Agric. Food Chem.* **2004**, *52*, 6042–6048. [CrossRef]
28. Friedman, M.; Henika, P.R.; Levin, C.E.; Mandrell, R.E. Antimicrobial wine formulations active against the foodborne pathogens Escherichia coli O157:H7 and Salmonella enterica. *J. Food Sci.* **2006**, *71*, 245–251. [CrossRef]
29. Vigni, M.L.; Durante, C.; Cocchi, M. Exploratory Data Analysis. *Chemom. Food Chem.* **2013**, *28*, 55–126. [CrossRef]
30. Bezerra, M.A.; Santelli, R.E.; Oliveira, E.P.; Villar, L.S.; Escaleira, L.A. Response surface methodology (RSM) as a tool for optimization in analytical chemistry. *Talanta* **2008**, *76*, 965–977. [CrossRef]
31. Lundstedt, T.; Seifert, E.; Abramo, L.; Thelin, B.; Nyström, Å.; Pettersen, J.; Bergman, R. Experimental design and optimization. *Chemom. Intell. Lab. Syst.* **1998**, *42*, 3–40. [CrossRef]
32. Leardi, E. Experimental design in chemistry: A tutorial. *Anal. Chim. Acta* **2009**, *652*, 161–172. [CrossRef] [PubMed]
33. Ding, X.; Guo, Y.; Ni, Y.; Kokot, S. A novel NIR spectroscopic method for rapid analyses of lycopene, total acid, sugar, phenols and antioxidant activity in dehydrated tomato samples. *Vib. Spectrosc.* **2016**, *82*, 1–9. [CrossRef]
34. Zhao, J.; Ouyang, Q.; Chen, Q.; Lin, H. Simultaneous determination of amino acid nitrogen and total acid in soy sauce using near infrared spectroscopy combined with characteristic variables selection. *Food Sci. Technol. Int.* **2013**, *19*, 305–314. [CrossRef]
35. *ISO 20645:2004*; Textile Fabrics—Determination of Antibacterial Activity—Agar Diffusion Plate Test. ISO: Geneva, Switzerland, 2004. Available online: https://www.iso.org/standard/35499.html (accessed on 16 October 2025).
36. Artajo, L.S.; Romero, M.P.; Suárez, M.; Motilva, M.-J. Partition of phenolic compounds during the virgin olive oil industrial extraction process. *Eur. Food Res. Technol.* **2007**, *225*, 617. [CrossRef]
37. Criado-Navarro, I.; Ledesma-Escobar, C.A.; Parrado-Martínez, M.J.; Marchal-López, R.M.; Olmo-Peinado, J.M.; Espejo-Calvo, J.A.; Priego-Capote, F. Monitoring the partition of bioactive compounds in the extraction of extra virgin olive oil. *LWT* **2022**, *162*, 113433. [CrossRef]
38. Koivikko, R.; Loponen, J.; Honkanen, T.; Jormalainen, V. Contents of soluble, cell-wall-bound and exuded phlorotannins in the brown alga fucus vesiculosus, with implications on their ecological functions. *J. Chem. Ecol.* **2005**, *31*, 195–212. [CrossRef]
39. Available online: https://foodb.ca/ (accessed on 1 December 2025).
40. Salvadeo, P.; Boggia, R.; Evangelisti, F.; Zunin, P. Analysis of the volatile fraction of 'Pesto Genovese' by headspace sorptive extraction (HSSE). *Food Chem.* **2007**, *105*, 1228–1235. [CrossRef]
41. D'Eusanio, V. Assessment of Lycopene Levels in Dried Watermelon Pomace: A Sustainable Approach to Waste Reduction and Nutrient Valorization. *Analytica* **2024**, *5*, 311–321. [CrossRef]
42. García-Salinas, S.; Elizondo-Castillo, H.; Arruebo, M.; Mendoza, G.; Irusta, S. Evaluation of the Antimicrobial Activity and Cytotoxicity of Different Components of Natural Origin Present in Essential Oils. *Molecules* **2018**, *23*, 1399. [CrossRef] [PubMed]
43. Persico, P.; Ambrogi, V.; Carfagna, C.; Cerruti, P.; Ferrocino, I.; Mauriello, G. Nanocomposite polymer films containing carvacrol for antimicrobial active packaging. *Polym. Eng. Sci.* **2009**, *49*, 1447–1455. [CrossRef]

44. Atarés, L.; Chiralt, A. Essential oils as additives in biodegradable films and coatings for active food packaging. *Trends Food Sci. Technol.* **2016**, *49*, 51–62. [CrossRef]
45. Flores, Z.; San-Martin, D.; Beldarraín-Iznaga, T.; Leiva-Vega, J.; Carvajal, R.V. Effect of Homogenization Method and Carvacrol Content on Microstructural and Physical Properties of Chitosan-Based Films. *Foods* **2021**, *10*, 141. [CrossRef] [PubMed]